SAND2015-8659J

Metal Hydride Differential Scanning Calorimetry as an Approach to Compositional Determination of Mixtures of Hydrogen Isotopologues and Helium

David B. Robinson, Weifang Luo, Trevor Y. Cai, and Kenneth D. Stewart
Sandia National Laboratories, PO Box 969 MS 9291, Livermore, CA, USA
Email: drobins@sandia.gov Phone: 1-925-294-6613 Fax: 1-925-294-3020

Gaseous mixtures of diatomic hydrogen isotopologues and helium are often encountered in the nuclear energy industry and in analytical chemistry. Compositions of stored mixtures can vary due to interactions with storage and handling materials. When tritium is present, it decays to form ions and helium-3, both of which can lead to further compositional variation. Monitoring of composition is typically achieved by mass spectrometry, a method that is bulky and energy-intensive. Mass spectrometers disperse sample material through vacuum pumps, which is especially troublesome if tritium is present. Our ultimate goal is to create a compact, fast, low-power sensor that can determine composition with minimal gas consumption and waste generation, as a complement to mass spectrometry that can be instantiated more widely. We propose calorimetry of metal hydrides as an approach to this, due to the strong isotope effect on gas absorption, and demonstrate the sensitivity of measured heat flow to atomic composition of the gas. Peak shifts are discernible when mole fractions change by at least 1%. A mass flow restriction results in a unique dependence of the measurement on helium concentration. A mathematical model is presented as a first step toward prediction of the peak shapes and positions. The model includes a useful method to compute estimates of phase diagrams for palladium in the presence of arbitrary mixtures of hydrogen isotopologues. We expect that this approach can be used to deduce unknown atomic compositions from measured calorimetric data over a useful range of partial pressures of each component.

Keywords: H2; D2; He; Pd; DSC; desorption

1. Introduction

The heavier isotopes of hydrogen are important in the operation of nuclear reactors, in studies of nuclear fusion, and in analytical methods such as gas chromatography and nuclear magnetic resonance spectrometry. In heavy-water reactors, presence of ^{1}H degrades reactor performance, and presence of radioactive ^{3}H is a safety hazard. Efforts are made to purify isotopic mixtures through water distillation, water electrolysis, methods based on absorption or adsorption, and hybrids of these. Hydrogen-helium mixtures result when ^{3}H decays to ^{3}He. Mixtures of $^{1}H_2$ and ^{4}He may be generated during gas chromatography if the carrier gas is varied. The increasing cost of helium is prompting recycling efforts, where characterization of mixture composition would be useful. Mixtures can also be generated during synthesis or reclamation of isotopically labeled organic compounds that are useful in nuclear magnetic resonance spectrometry.

Currently, mass spectrometry is the main method to determine the composition of gaseous mixtures of hydrogen isotopologues and helium.[1,2] Mass spectrometers are bulky, expensive, and energy intensive, and they require vacuum maintenance. This is especially onerous when tritium is used, requiring handling of dilute radioactive pump exhaust, and periodic disposal of worn out pump components that have radioactive contamination. Some commercial quadrupole mass spectrometers have difficulty distinguishing species of similar mass such as $^{2}H_2$ and ^{4}He, or the diatomic molecule $^{1}H^{2}H$ and ^{3}He. Finite filter bandwidths, and generation of minor species such as H_3^+, limit the ability to measure trace species in a mixture.

If composition could be measured by a method that is more compact and lower power, without consuming or dispersing the sampled gas, it will be possible for a gas handling system to report composition at more sampling points, allowing deviations from target values to be corrected before they propagate to other parts of the system, improving system reliability and safety, and improving efficiency of gas use.

Calorimetry is an experimental technique that has been successfully miniaturized in the form of sub-millimeter, sub-milliwatt sensors.[3,4,5] We desire to adopt this method for use in processes involving the hydrogen isotopologues and helium. With a compact sensor for these gases, the composition of process gases can be known and controlled at a larger number of points throughout a system, improving reliability of process operations, without incurring the cost of bulky component disposal after replacement. In this report, we focus on study of milligram-scale palladium samples in the presence of varying gas mixtures using a commercial differential scanning calorimeter. This has allowed us to determine the basic chemical and physical sensing characteristics. For hydrogen detection, we rely on the sensitive isotopic dependence of the temperatures of hydrogen absorption and desorption by palladium. This dependence is primarily on atomic composition, and does not easily reveal how the gas-phase isotopes are arranged as diatomic isotopologues, but the atomic composition is still useful information. The approach can resolve mixtures of two different isotopes, but not all three; we focus on ^{1}H and ^{2}H here. To determine the amount of helium, we rely on its mass transport effects in the presence of a flow restriction. A satisfactory model of the system is constructed using simple assumptions about mass transport and the metal hydride phase behavior. In principle, this model could be used to determine previously unknown atomic compositions from experimental data, which would be necessary for the development of a practical sensor.

Scanning calorimetry in hydrogen atmospheres has proven to be a valuable technique in the study of solid-phase hydrides and deuterides such as those of palladium,[6,7] palladium alloys,[8,9] magnesium alloys and compounds,[10,11,12] and lanthanum alloys,[13] so there is precedent for our experimental methods. The behavior of metal hydrides in mixtures of hydrogen isotopologues [14,15,16,17] and inert gases [18] has also been studied. This prior work adds confidence that our proposed approach can be understood in detail. A significant body of prior knowledge of palladium hydride thermochemistry [19] and the demonstration of the high reversibility of palladium to hydriding and dehydriding cycles [20] motivated our choice of palladium as a sorbent material in this work.

2. Materials and Methods

The commercial calorimeter used is the Mettler Toledo HP DSC 1, which is essentially a differential scanning calorimeter mounted inside a pressure vessel. The instrument comes with a mass flow control module that was bypassed for our studies. The palladium (Pd) powder was purchased from Engelhard, and has a surface area of about 1 m^2/g. This corresponds to a particle size of about 0.3 µm, assuming the particles are spheres. A sample of about 10 mg Pd powder is placed in a 40-microliter aluminum pan, and a lid with a 50 micrometer diameter laser-drilled hole is crimped onto the pan to form a capsule. The Pd mass for the data presented here is 11.1 mg. An empty capsule with a similar hole is used as a reference. These capsules are placed side by side on a heater-thermocouple assembly that is mounted in the pressure vessel, which has an operating range from 0 (vacuum) to 10 MPa. As a cleaning procedure, an air-exposed Pd sample is heated to 150 °C and cycled 3 times between vacuum and several tens of kPa H_2 prior to any calorimetry experiments.

The instrument was calibrated by performing calorimetry experiments with a capsule containing about 6 mg indium in the presence of helium. The instrument software uses the known melting point and enthalpy of indium to determine the temperature and heat flow scales. A time lag correction that partially compensates for the finite response time of the system is also made by performing this calibration at several scan rates.

A homemade gas manifold was fabricated to deliver gas to the pressure vessel. The manifold allows argon, hydrogen, gas from an auxiliary port, and vacuum to be applied to the pressure vessel. Vacuum is provided by a rotary vane pump. The auxiliary gas is typically helium or deuterium in a 1-liter pressure vessel at 200 psi, with its own regulator. The manifold is equipped with a 100 psi pressure transducer, 90 psi pressure relief valve, and a vacuum gauge that measures to the millitorr range. Pneumatic valves and interlocked switches control gas flow on the front panel. The auxiliary gas port is controlled through a manual valve. The argon is used only to fill the chamber prior to opening it to change samples. Gas mixtures were prepared by dosing a given pressure of a first gas to the chamber, followed by a dose of a second gas to the desired total pressure, and then waiting at least 30 minutes for gases to mix. Experiments performed after this amount of time give essentially the same result as experiments performed with longer mixing times.

We refer interchangeably to ^{1}H and H, and ^{2}H and D (deuterium). However, *T* refers to absolute temperature, and not tritium.

3. Theory

3.1 General Approach

At high temperatures or low pressures, palladium absorbs only a small amount of hydrogen, which forms a dilute solution of interstitial hydride, known as the alpha phase. At a specific temperature for a given pressure (or a specific pressure for a given temperature), a phase change occurs (assuming the temperature is below about 300 °C) where the palladium absorbs to a much higher concentration of hydrogen, and the metal lattice expands. This is known as the beta phase. In previous studies, this is usually reported as a pressure-composition isotherm as a function of temperature and isotope, for pure isotopes.[21,22] The case of mixed isotopologues has been addressed by prior Sandia work,[17] and will be discussed below. The experiments to generate these isotherms chart an orthogonal path in phase space versus the calorimetry experiment. For a pressure-composition isotherm, the temperature is held constant, and the pressure is ramped. For calorimetry, the pressure is held constant, and the temperature is ramped.

In a typical calorimetry experiment reported here, the temperature is ramped linearly from slightly above room temperature to a higher temperature, held there briefly, and then ramped back to room temperature. The excess amount of power needed to maintain this temperature program, as compared to a reference capsule, is recorded. Ramp rates are 2 to 20 °C per minute, and upper temperatures range from 120 to 250 °C. The assembled sample capsule is illustrated in Figure 1. When there is a change in the amount of hydrogen in the solid phase, gas will flow through the pinhole. Due to this mass flow restriction, the partial gas pressures inside the capsule can be expected to temporarily differ from the outside environment. Understanding this difference will allow us to deduce the helium partial pressure, even though this component is not absorbed by the palladium.

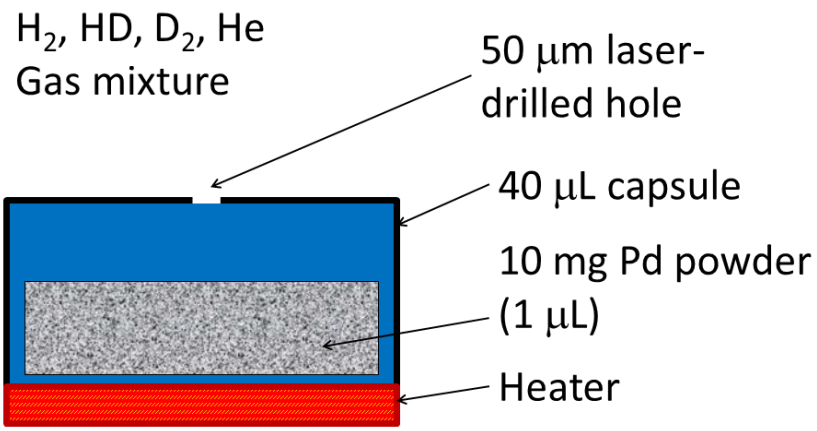

Figure 1. Schematic of palladium-containing calorimetry capsule on heater-thermocouple assembly. The dimensions and mass in this figure are meant to be approximate.

In principle, calorimetry of a palladium sample of this geometry could be used as a sensor by empirically tabulating peak positions for many gas compositions. It is still necessary to have a separate measurement of the total pressure so that measured peak positions can be compared to the positions expected for the pure gas at that pressure. The effect of helium can be distinguished because it results in a significant separation of the peaks. However, a purely empirical approach will require a substantial amount of data collection, and the data would not be valid if we change the amount of palladium, the volume of the sample capsule, or the size of the hole. To make more robust predictions of experimental results under given experimental conditions, and eventually be

able to deduce the experimental conditions from the results, we have created a simple mathematical model of the experiment. There is precedent for modeling differential scanning calorimetry experiments, including pioneering work,[23,24] theoretical studies,[25,26,27] reviews,[28,29] and computer simulations.[30,31] However, we have not found prior models in the literature that involve reactions with gas-phase species.

We simulate the experiment in GNU Octave, a free and open source software package that is similar to Matlab, using its built-in ordinary differential equation solver, LSODE.[32] Our model makes numerous assumptions that are rather crude. The intent of this effort is to determine the simplest assumptions necessary to describe our observations, evaluate the validity of those assumptions, and provide a basis for further elaboration.

3.2 Mass balance and mass transport

Figure 2 depicts the variables involved in the model. The gas composition in the chamber is considered fixed. The amounts of hydrogen, deuterium, and helium inside the capsule can vary with time. Here, we do not explicitly keep track of the mixed isotopologue HD, but assume it is in chemical equilibrium with the other gases, and offer a way to indirectly account for it. The amounts of hydride and deuteride in the solid can also vary, although we will assume that they are always close to equilibrium with the gas composition inside the capsule. We will assume that gases can be transported between the capsule and chamber according to either a simple pressure-driven flow model, or by a simple diffusion law.

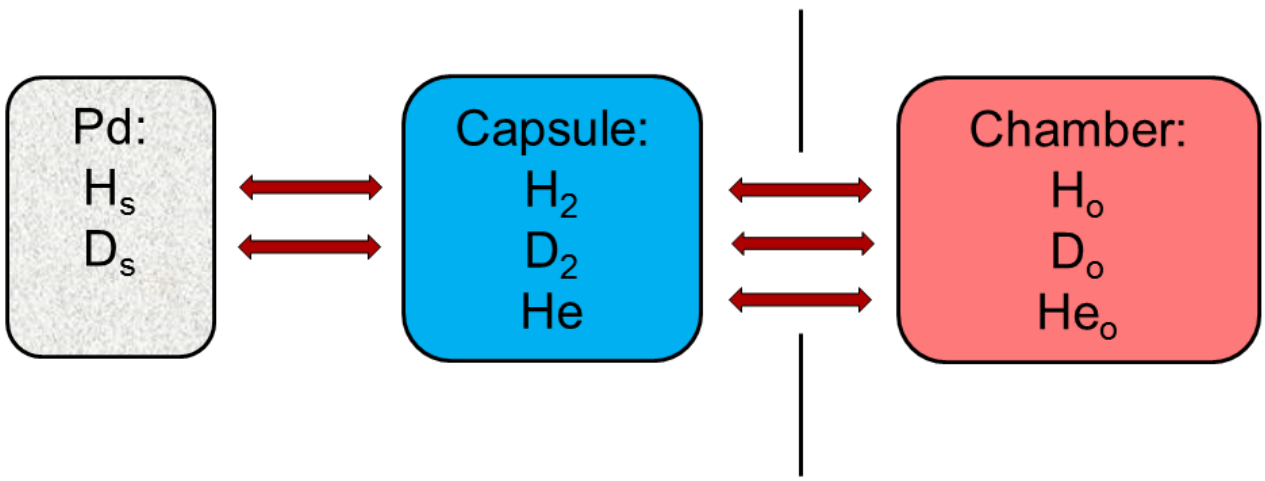

Figure 2. Species accounted for by the model of the Pd capsule, for each of three regions: within the palladium, within the capsule, and in the pressure vessel (chamber) outside of the capsule. Arrows represent transport laws that are formulated between each region.

A set of first-order differential equations describing transport between the regions includes a set for the gas-phase species, including a term for pressure-driven flow through the hole, a term for diffusion through the hole, and a term for absorption or desorption with the solid. There are two versions of the equations for the gas-phase species, depending on the flow direction. When gas is flowing into the capsule,

$$V\frac{dH_2}{dt}=\frac{\pi r^4}{8\mu L}\frac{H_o}{n_o}\left(n_o RT_o-nRT\right)+\frac{D_{\mathrm{H}}\pi r^2}{L}\left(H_o-H_2\right)-km\left(H_2-H_{eq}\right) \quad (1)$$

$$V\frac{dD_2}{dt}=\frac{\pi r^4}{8\mu L}\frac{D_o}{n_o}\left(n_o RT_o-nRT\right)+\frac{D_{\mathrm{D}}\pi r^2}{L}\left(D_o-D_2\right)-km\left(D_2-D_{eq}\right) \quad (2)$$

$$V\frac{dHe}{dt}=\frac{\pi r^4}{8\mu L}\frac{He_o}{n_o}\left(n_oRT_o-nRT\right)+\frac{D_{\mathrm{He}}\pi r^2}{L}\left(He_o-He\right) \tag{3}$$

where t is time; V is the volume of the capsule (its empty volume minus the volume of the Pd, which is assumed constant); H_2, D_2, and He are the concentrations of these gas species in the capsule; n is the sum of these; H_o, D_o, and He_o are the fixed concentrations of hydrogen, deuterium, and helium outside of the capsule; n_o is the sum of these; H_{eq} and D_{eq} are the values of H_2 and D_2 that would be at equilibrium with the solid; T_o is the absolute temperature outside of the chamber; D_H, D_D, and D_{He} are gas-phase diffusion constants for each species; μ is the viscosity of the gas mixture in the chamber; r is the radius of the hole in the capsule; L is the thickness of the lid; k is a chemical rate constant for adsorption and desorption; and m is the number of moles of palladium in the capsule. When gas is flowing out of the capsule ($nRT > n_oRT_o$), the mole fractions in the flow term are for the gas inside the capsule instead of outside:

$$V\frac{dH_2}{dt}=\frac{\pi r^4}{8\mu L}\frac{H_2}{n}\left(n_oRT_o-nRT\right)+\frac{D_{\mathrm{H}}\pi r^2}{L}\left(H_o-H_2\right)-km\left(H_2-H_{eq}\right) \tag{4}$$

$$V\frac{dD_2}{dt}=\frac{\pi r^4}{8\mu L}\frac{D_2}{n}\left(n_oRT_o-nRT\right)+\frac{D_{\mathrm{D}}\pi r^2}{L}\left(D_o-D_2\right)-km\left(D_2-D_{eq}\right) \tag{5}$$

$$V\frac{dHe}{dt}=\frac{\pi r^4}{8\mu L}\frac{He}{n}\left(n_oRT_o-nRT\right)+\frac{D_{\mathrm{He}}\pi r^2}{L}\left(He_o-He\right) \tag{6}$$

where the viscosity is assumed to be the same as for the gas that flows in. Equations for the rate of change with time of H and D are

$$m\frac{dH}{dt}=2km\left(H_2-H_{eq}\right) \tag{7}$$

$$m\frac{dD}{dt}=2km\left(D_2-D_{eq}\right) \tag{8}$$

where H and D are the concentrations of these isotopes in the palladium in moles per mole Pd, and the factor of 2 accounts for the fact that two hydrides are created for every absorbed diatomic gas molecule. While H and D do not appear explicitly in the gas-phase equations, those equations do depend on H_{eq} and D_{eq}, which in turn depend on H and D.

The pressure-driven flow model is that of a pipe with laminar flow. This is a reasonable starting point given that the hole depth exceeds its diameter. The Reynolds number under these conditions is about 5, so the model is not expected to be perfect, but the simplicity of the model makes it a reasonable starting point. Diffusion through the hole is modeled by Fick's law for one dimension at steady state, where the molar transport rate is directly proportional to the diffusion constant and hole area, and inversely proportional to hole depth. The diffusion constants are expected to depend on molecular weight, pressure, and temperature, but in this work they are all taken to be 1 cm^2/s, which is close to their values at room temperature and pressure. The value of k was made large enough to ensure that the result is not very sensitive to this parameter, but not so large that the simulation does not converge.

3.3 Thermodynamics of absorption and desorption

Several previously reported approaches are available to compute H_{eq} and D_{eq}. The problem was first addressed many decades ago.[33] Several sophisticated models have been reported recently, but are relatively difficult to implement in the present context.[34,35] We rely on a combination of previously reported methods, primarily by Oates, Lässer, Kuji, and Flanagan.[36,37] These methods allow us to account for the thermodynamic effect of mixed isotopologues such as HD. At equilibrium, the chemical potentials of H and D in the solid are equal to those of the diatomic gas-phase molecules that contain them:

$$\mu_{ij}^{g} = \mu_i^s + \mu_j^s \tag{9}$$

where *i* and *j* represent a hydrogen isotope (^{1}H or ^{2}H), μ_i^s is the chemical potential of one such isotope in the solid, and μ_{ij}^g is the chemical potential of the gas-phase diatomic species containing *i* and *j*. Equation 12 is actually a set of three equations for the three combinations of *i* and *j*. The three gas-phase chemical potentials can be related to their partial pressures and a standard-state term μ_{ij}^0 that is independent of pressure:

$$\mu_{ij}^{g} = \mu_{ij}^0 + RT\ln\left(P_{ij}/1\,\text{atm}\right) \tag{10}$$

The standard-state term is a complicated function of temperature, *i* and *j*, and is given by the right-hand side of equation 10 and Table I in Ref. 38. It captures the translational, vibrational, and rotational partition functions of the gas-phase species, as well as the bond dissociation energies.

The solid-phase chemical potential can similarly be described as a composition-dependent standard-state term μ_i^0, a term capturing the entropy of mixing, and an "excess" chemical potential μ^{ex} that depends on composition.

$$\mu_i^s = \mu_i^0 + RT\ln\left(\frac{x_i}{x_v}\right) + \mu^{ex} \tag{11}$$

where x_i is either *H* or *D*, and $x_v = 1 - H - D$. The excess chemical potential, in J/mol, is extracted from Ref. 39, Equation 28:

$$\begin{aligned}\mu^{ex} = &\left(-68555 + 51.57T\right)(H+D)\\ &+\left(6463449 - 79.31T\right)(H+D)^2\\ &+\left(2435539 - 23.667T\right)(H+D)^3\end{aligned} \tag{12}$$

This function was apparently derived from fits to pressure-composition isotherms in the fully hydrided (β phase) region, subject to the constraint that the function is zero when *H* and *D* are zero. The excess chemical potential captures the electronic and elastic effects that oppose the occupancy of all octahedral sites within the Pd lattice by a hydrogen isotope. It is assumed here that the excess chemical potential is isotope-independent, which simplifies the determination of the equilibrium concentrations.

The standard-state chemical potential is given by

$$\mu_i^0 = -RT\ln\left[\frac{1 + A_i\exp\left(-B_i/T\right)}{\left(1-\exp\left(-C_i/T\right)\right)^3}\right] - R\left(E_i - \tfrac{3}{2}C_i\right) \tag{13}$$

where A_i, B_i, C_i, and E_i are found in Table II of Ref. 38. This formula is a simplication of Ref. 38 that is provided in Ref. 37. It captures a model for the vibrational partition function of the solid-phase hydrides along with the absorption enthalpy. References 36-39 contain information allowing extension of this approach to include tritium.

The desired values of H_{eq} and D_{eq} can be derived from

$$H_{eq} = \frac{P_{HH}}{RT} + \frac{P_{HD}}{2RT} \tag{14}$$

$$D_{eq} = \frac{P_{DD}}{RT} + \frac{P_{HD}}{2RT} \tag{15}$$

after solving the above equations for the partial pressures. This approach applies when the palladium is in the fully hydrided state (β phase) or fully dehydrided state (α phase). It does not capture the mixed-phase region, a pressure plateau in the pressure-composition isotherm where the equilibrium pressure is independent of composition; this requires further consideration.

3.4 Plateau pressures

The dependence of the plateau pressures on temperature is described by Lässer and Klatt.[40]

$$\frac{P}{1\,\mathrm{bar}} = \exp\left(-\frac{\Delta H - T\Delta S}{RT}\right) \tag{16}$$

where P is the pressure, T is the absolute temperature, ΔH is an empirical enthalpy, ΔS is an empirical entropy, and R is the ideal gas constant. Solving for T gives

$$T = \frac{\Delta H}{\Delta S - R\ln(P/1\,\mathrm{bar})} \tag{17}$$

The values of the empirical enthalpies and entropies are sample-dependent, because samples of different geometry and microstructure exhibit different amounts of hysteresis. We have determined values based on our own experimental calorimetry of the pure gases, as described below.

In the mixed-phase region, the computed partial pressures exhibit both a maximum and a minimum as a function of solid-phase composition. These are shown in Figure 3 as pressure-composition isotherms for a case that is nearly pure hydrogen. Also shown are the absorption and desorption pressures as predicted by our empirical fits, shown has horizontal lines. As the occupied mole fraction increases from zero, a physically plausible isotherm would follow the total pressure curve up to the absorption pressure, remain at that pressure until the total pressure curve crosses above it a second time, and then follow the total pressure curve up to high occupied mole fractions. As the occupied mole fraction decreases from a high value, the isotherm would follow the total pressure curve down to the desorption pressure, remain at that pressure until the total pressure curve crosses below it a second time, and then follow the total pressure curve down to low occupied mole fractions. This approach can give a complete isotherm for the case of pure gases, but Lässer and Klatt do not offer a prediction of plateau pressures for gas mixtures. For an arbitrary composition, W. G. Wolfer [37] recommended in a personal communication that we use a Maxwell construction, where the pressure in the mixed-phase region is one that bounds an equal area of the total pressure curve above and below the line. This left open the question of how to apply hysteresis to obtain the absorption and desorption pressures. We were not able to reconcile computed Maxwell constructions with the Lässer and Klatt pressures in a straightforward way. Instead, we compared the trough pressures to plateau pressures derived from our experimentally measured adsorption onsets for pure gases, and created an exponential fit to the ratio of these pressures as a function of reciprocal temperature. The quality of the fits are illustrated in Figure S1 of the Supplementary Material. The calculated plateaus were constrained to be between the peak and the trough. Examples of the calculated plateaus are shown in Figure 3, and closely match the experimental values at this temperature. This approach has the added advantage that it is easier to calculate. A Maxwell construction requires numerical integration of the entire total pressure curve through evaluation at a large number of points, whereas the peak and trough can be identified by a relatively small number of iterations of the Newton-Raphson method.

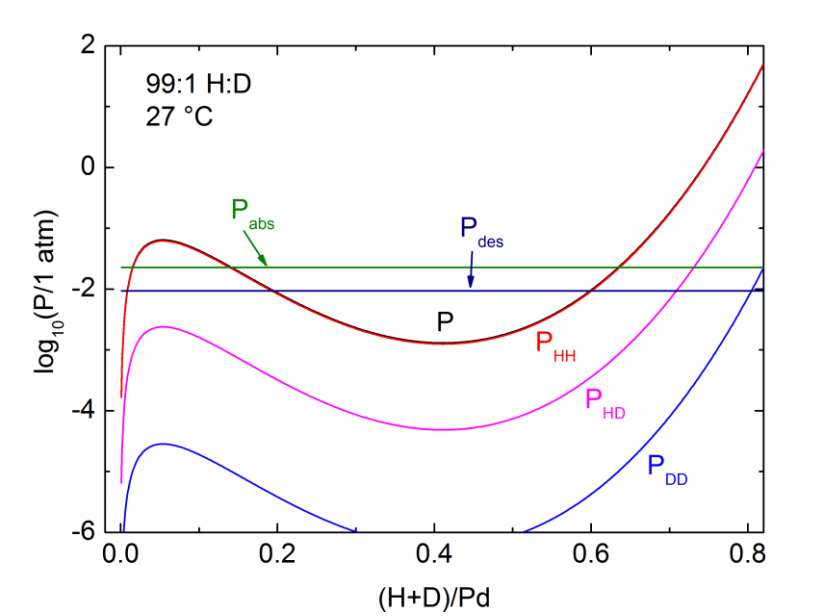

Figure 3. Plots of the partial pressures of the diatomic species, and the total pressure, as a function of H+D for a fixed H:D ratio of 99:1, as calculated by Equations 11-17. Also plotted are estimates of the absorption and desorption pressures, based on an empirical correlation to the minimum of the total pressure.

Figure 4 shows a family of pressure-composition isotherms predicted by this approach for a mixed gas composition at a series of temperatures. The curve shapes resemble the typical shapes of pure-gas isotherms, approaching a critical point at about 300 °C, above which the mixed-phase region does not exist. Gathering experimental data to validate these predictions would be challenging, because it is difficult to monitor the isotopic composition in the solid and maintain a constant H:D ratio. However, this approach can still be applied in our model to predict and interpret calorimetry data.

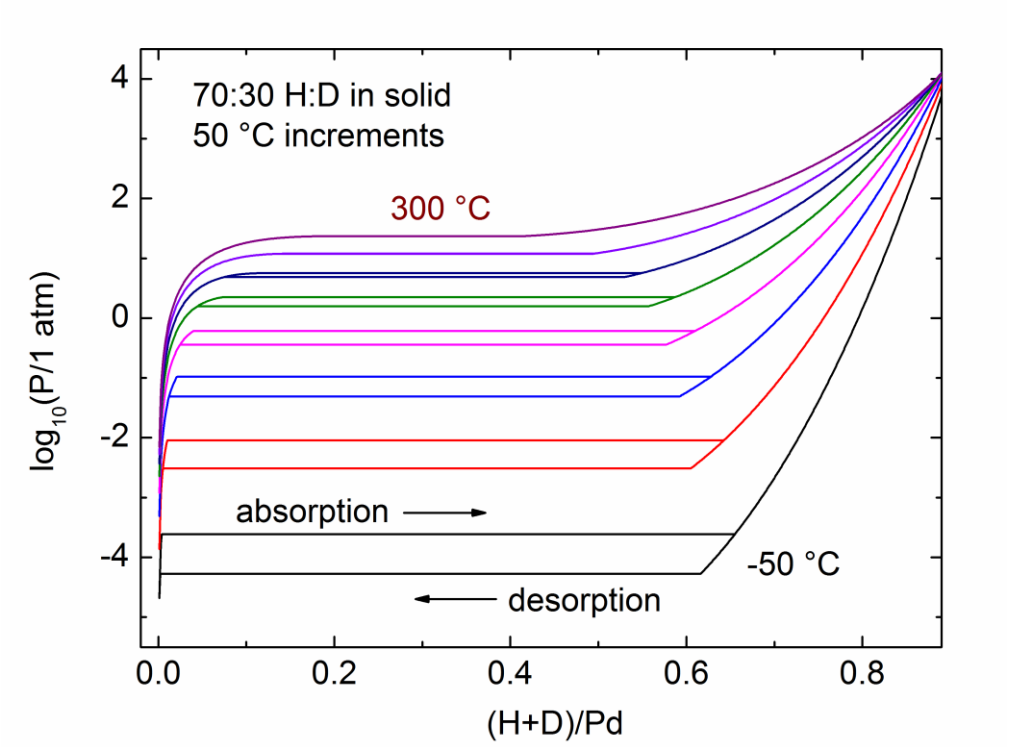

Figure 4. Predicted pressure-composition isotherms, including both absorption and desorption traces, when the ratio of H:D in the solid is fixed at 70:30, for a series of temperatures at 50 °C intervals from -50 to 300 °C.

3.5 Heat flow calculations

The heat flow is computed by multiplying half of the appropriate enthalpy per H_2 or D_2 molecule, as derived from our Lässer and Klatt fits, by the respective rates of change of *H* or *D* with time, using the absorption enthalpy when the rate is positive and the desorption enthalpy when the rate is negative. A contribution due to heat capacity was computed by multiplying the temperature scan rate by the present amounts of gases, Pd, and hydride by their room-temperature literature values of constant-pressure heat capacity. A contribution due to the heating of incoming gas from room temperature to the sample temperature was computed by multiplying the flow rate of each gas species into the pan (the first two right-side terms of Equations 3-5) by the heat capacity of each species and the temperature difference $T - T_o$.

4. Results

4.1 Calorimetry of pure gases

In a calorimetry experiment, upon ramping from low to high temperatures, we expect to see a sharp absorption of heat (negative heat flow) at the gas desorption temperature. When subsequently ramping from high to low temperatures, we expect a sharp release of heat (positive heat flow) when gas is absorbed. Figure 5 shows measurements made in the presence of several pressures of pure hydrogen or pure deuterium at a slow

temperature scan rate (2 °C/min). Each measurement shows a desorption peak that occurs at a higher temperature than the absorption peak. This hysteresis is from the same effect that causes the pressure hysteresis in the isothermal experiment modeled in Figure 4, but the order is reversed; in that case, desorption occurs at a lower pressure than absorption. The effect is generally recognized as due to the additional work required to plastically deform the palladium during the lattice expansion that accompanies absorption, and the contraction when the gas desorbs.[41] Because absorption of hydrogen is more thermodynamically favorable than the absorption of deuterium, the hydrogen absorption and desorption peaks occur at higher temperatures for a given pressure.

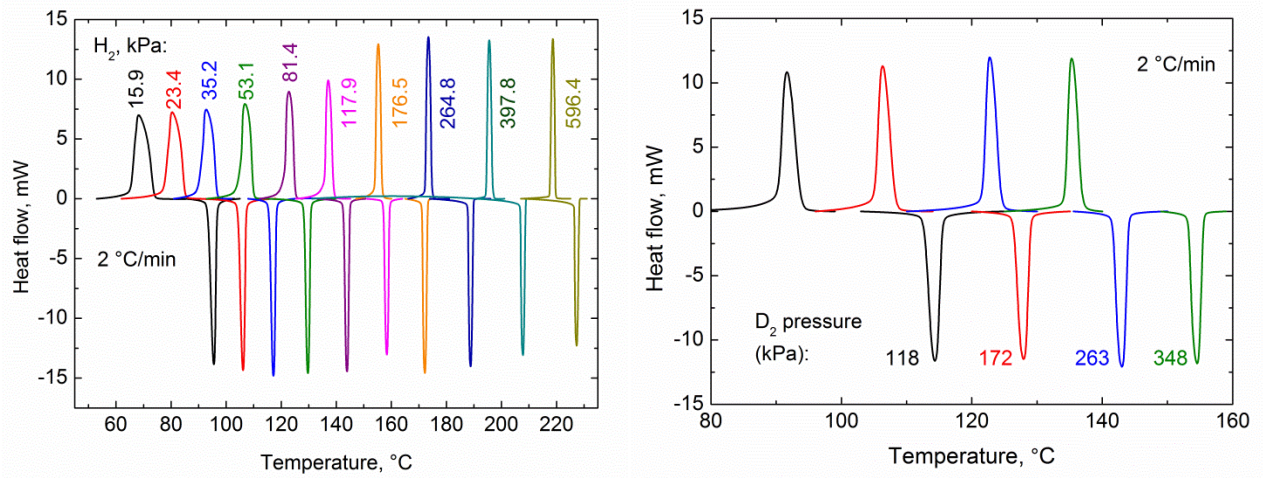

Figure 5. Peaks in heat flow to the sample measured during differential scanning calorimetry of the Pd sample in the presence of various pressures of (left) hydrogen and (right) deuterium gas.

The peaks are superimposed on a nonzero baseline, as shown in Figure S2 in the Supplementary Material. This baseline corresponds to the difference in heat flow between the sample and reference capsule. The baseline can vary as a function of temperature and gas environment, and can arise from various instrumental factors. In the experimental data presented in this paper, baselines have been established by connecting two points far from each peak with a straight line, and have then been subtracted from the data. This correction facilitates comparison of the positions and shapes of peaks measured under different conditions.

The onset temperatures for each peak in Figure 5, made by extrapolations of linear fits of the rising side of each peak to the baseline, were fit to Equation 16. Plots of these fits appear in Figure S3 of the Supplementary Material, and the derived enthalpy and entropy values are reported in Table 1.

	ΔH, kJ/mol		ΔS, J/mol K	
	H	D	H	D
Desorption	40.9	36.1	96.8	95.3
Absorption	34.9	31.9	85.6	87.9

Table 1. Enthalpy and entropy parameters for prediction of desorption and absorption temperatures and pressures, based on fits to the onset temperatures in Figure 5. The units are in moles of diatomic gas.

The areas under the curves (plotted versus time instead of temperature) are expected to correspond to the product of the enthalpy of the transition as described in Table 1, multiplied by the hydride occupancy difference between the hydrided (beta) and dehydrided (alpha) phases, expressed as a number of moles of gas. The areas

under each curve in Figure 5 are about 0.57 J for desorption and 0.65 for absorption of hydrogen. For deuterium, the values are 0.58 J for desorption and 0.68 J for absorption. Given that we have 0.104 mol Pd, that the composition difference between phases is about 0.5 mol H/mol Pd, and there are 0.5 mol H_2/mol H, we compute enthalpies of about 24 kJ/mol H_2, notably lower than the values in Table 1.

Several effects may degrade the trustworthiness of measured enthalpy values. The enthalpy calibration is sensitive to thermal transport near the capsules. When palladium absorbs and desorbs hydrogen, about 25 micromoles of the gas (about 800 microliters or 20 times the capsule volume at 100 kPa) enters and leaves through the hole – an effect that is not present during calibration with indium. This gas motion can affect heat transport. Thermal conductivity varies slightly with composition, temperature and pressure. Also, the gas must be heated from room temperature upon absorption, which can account for a few kJ/mol. As with the baselines, we will mostly ignore the absolute peak areas and instead focus our investigation on peak position and shape. Prior studies have shown that reliable enthalpy values can be determined when the gas environment and other experimental factors are well known and controlled.[9,12].

The hydrogen plot includes several pressures that are lower than those shown for deuterium. There is a notable broadening of the absorption peaks at those pressures. We attribute this to slower absorption kinetics at the lower temperatures involved. At the highest temperatures, hydrogen is absorbed by the sample in about 1 minute, whereas about 5 minutes is required at the lowest temperatures.

More generally, the peaks will have a finite width that depends on temperature scan rate, as shown in Figure 6. The areas under the heat flow-versus-time curves are approximately the same, because the transition enthalpies are expected to be constant. To arrange so that the areas are approximately constant when plotted versus temperature, the heat flow values are divided by scan rate in Figure 5. The peaks are broader at higher scan rate. These experiments were performed at a relatively high pressure, so that the peak temperatures are high, and absorption/desorption kinetics are presumably fast. The overall process that produces the peak can still be slow, because the gas must enter and exit through the flow restriction at a finite rate.

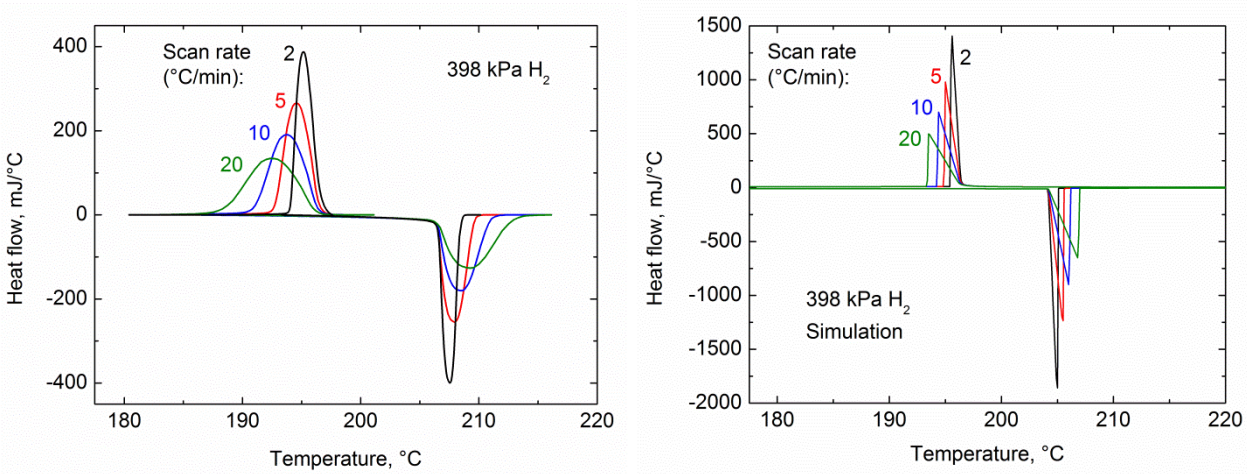

Figure 6. (Left) Peaks from a series of calorimetry experiments measured at a constant hydrogen pressure, but varying temperature scan rate. (Right) Simulations of the experiments. Heat flow is divided by scan rate so that peaks have similar areas.

As the gas desorbs from the palladium, the gas pressure inside the sample may increase before it can equilibrate with the pressure outside the sample through transport of gas through the hole in the lid. This increases the equilibrium desorption temperature, requiring an increase in temperature before more gas desorbs. The overall effect is that the peak is broader when gas must go through the flow restriction more quickly. The reverse is expected during absorption: uptake of the gas reduces the pressure in the sample if that uptake rate is faster than

the rate of gas flow through the hole, causing a reduction of the equilibrium absorption temperature as absorption proceeds, thus broadening the peak.

The shapes of the simulated peaks in Figure 6 are sharper, probably because the simulations do not capture aspects of the heating and measurement response times of the calorimeter. The areas under the curves are higher than the experimental data, reflecting the discrepancy noted earlier that we believe is related to our method of calibration of the instrument. The peak onsets are close to those predicted by the Table 1 fits, and are within a few degrees of the experimental data. The simulation captures the peak broadening trend qualitatively; a more detailed investigation of the relative contributions of absorption-desorption kinetics, mass transport, and instrumental effects could lead to a more quantitatively accurate simulation.

4.2 Calorimetry of hydrogen-helium mixtures

The above results outline the behavior of single-component gases (pure H_2 or pure D_2) in calorimetry experiments. Multi-component gases show significant differences in calorimetry results. These can be used to deduce atomic composition in the gas phase.

The simplest example of this is a mixture of hydrogen and helium. Figure 7 demonstrates the effect of adding increasing amounts of helium to the pressure vessel. There is a significant shift in peak position and shape, though the peak onset does not change. Baseline correction is also required in the case of gas mixtures; an example is shown in Figure S4 of the Supplementary Material. As noted for the case of Figure 6, the hole in the sample lid creates a mass transport limitation that can cause the pressure inside the sample to differ from the pressure outside. When helium is present, there can also be a difference in composition. During desorption, only hydrogen comes out of the palladium, whereas both hydrogen and helium exit through the hole. The partial pressure of hydrogen can thus increase significantly, increasing the desorption temperature corresponding to equilibrium between the palladium and the gas inside the capsule. The peak thus shifts toward a temperature corresponding to a hydrogen pressure equal to the total pressure. During absorption, the palladium absorbs only hydrogen, but a mixture of both hydrogen and helium flows through the hole. This causes helium to accumulate until its partial pressure inside the capsule approaches the total pressure. The absorption temperature corresponding to equilibrium between the palladium and the hydrogen partial pressure inside the capsule then decreases. We expect that pressure-driven flow through the hole is mostly stopped by the accumulation of helium, and heat flow is limited by diffusion of hydrogen through the hole. Figure 7 shows that, at 2 °C/min, the peak resulting from 1% He in H_2 is distinguishable from 0%. We suggest that this is approximately the detection limit for helium in a mixture with hydrogen.

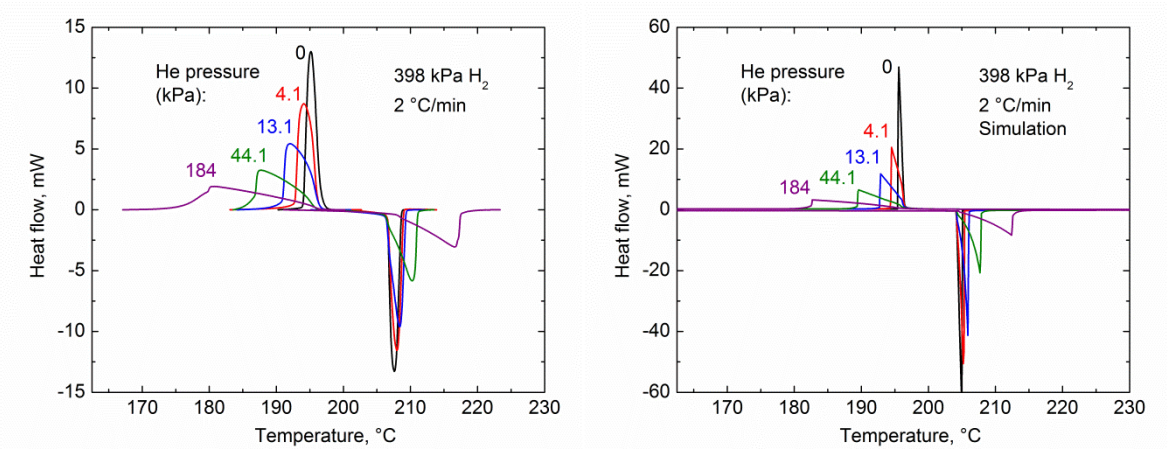

Figure 7. (Left) Effect on hydrogen calorimetry peaks of adding increasing amounts of helium. (Right) Simulations of the experiments.

As for the case of pure hydrogen, the simulated peak positions are a few degrees different from the experiments, and the simulated areas are higher. The shapes of the simulated peaks are sharper, but their widths follow a trend similar to those of the experiments, and the peak shapes show the same gradual increase followed by a sharp drop. The absorption peaks are broader than the desorption peaks, as was observed in the experiment. The predicted detection limit appears to be close to 1% He in H_2, also consistent with the experiment.

The sensitivity to helium may be different at different scan rates. Figure 8 shows the effect of varying scan rate for a case where there is a relatively large mole fraction of helium. The desorption peak shifts and broadens slightly as scan rate increases. The absorption peak shape is very sensitive to the presence of helium, and to the scan rate, due to the strong blanketing effect of the helium during absorption, and the mass transport limitation on hydrogen transport in the presence of this blanket. For a given set of conditions, there is presumably an optimal scan rate where the blanketing effect is strong enough to clearly distinguish a peak from cases with more or less hydrogen, but not so extreme that the peak does not fit into the available temperature range.

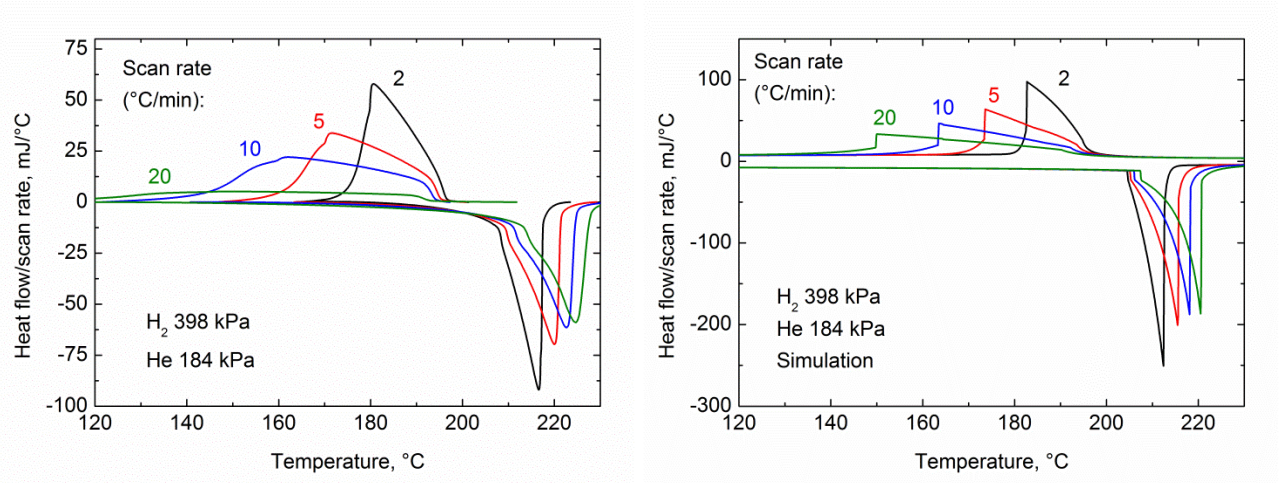

Figure 8. (Left) Calorimetry peaks for hydrogen absorption and desorption in the presence of a large mole fraction of helium. (Right) Simulations of these experiments. The plots are normalized by scan rate, as in Figure 6.

The scan rate dependence shown in Figure 8 is also qualitatively well reproduced by the simulation. Similar peak shapes and widths are observed for each scan rate. An offset is apparent in the simulation due to the inclusion of heat capacity in the model. Any such offset in the experimental data is removed by background subtraction.

A plot of the gas concentrations in the capsule during the 10 °C/min simulation in Figure 8 is shown in Figure 9. It illustrates how the peak shifts occur. There is a gradual decrease in both gas concentrations with temperature due to thermal expansion. Superimposed on this are significant excursions from the initial pressure ratio. During desorption, the gas composition inside the capsule becomes almost all hydrogen, as the initial gas mixture in the capsule is displaced. The accumulation of hydrogen in the capsule shifts the desorption temperature to a slightly higher value, slowing the desorption and broadening the peak. When the hydrogen has been depleted from the palladium, the heat flow abruptly drops. The gas concentration in the capsule equilibrates more slowly as helium diffuses back in. During absorption, the hydrogen concentration falls as the helium blanket forms. The absorption temperature decreases due to the decreased hydrogen concentration, slowing the process, but enough hydrogen still enters through flow and diffusion that the palladium eventually fills. This point corresponds to the sharp corners on the concentration peaks in Figure 9, and the abrupt drop at the end of the heat flow peak in Figure 8. After this, hydrogen continues to diffuse into the capsule, restoring compositional equilibrium with the gas outside the capsule. The difference between the absorption and

desorption peak shapes is due to the greater reliance on diffusion to supply hydrogen to the sample during absorption, and a greater reliance on flow to remove the hydrogen during desorption.

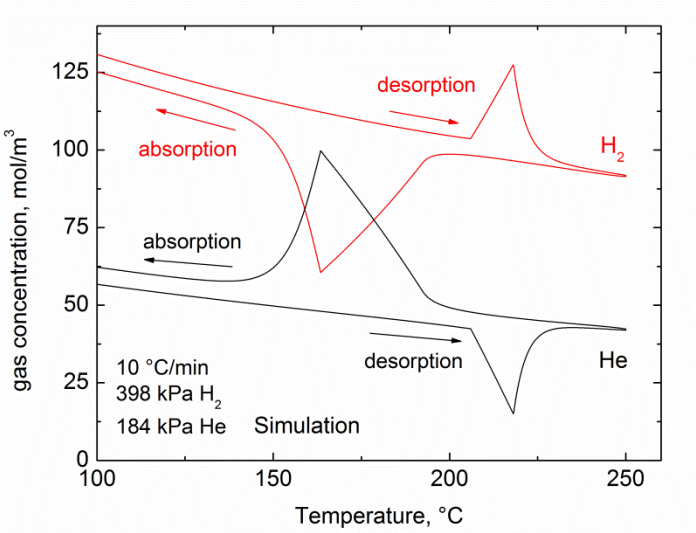

Figure 9. Hydrogen and helium concentrations in the capsule for the 10 °C/min simulation in Figure 8.

4.3 Calorimetry of hydrogen-deuterium mixtures

When small amounts of deuterium are added to hydrogen, the results are quite different from the previous cases. Figure 10 shows that the peak positions initially do not change. The increased deuterium content acts to reduce the peak temperatures, whereas the increased total pressure acts to increase peak temperatures, so the net change is small. Absorption of deuterium into palladium is not as thermodynamically favorable as for hydrogen, but the deuterium can still be absorbed, and it does not behave like an inert gas. Adding 54.5 kPa D_2 to 119 kPa H_2 shifts the peak temperatures by about 5 °C. However, that shift is much less than would be obtained by adding a similar amount of hydrogen. Figure 5 shows that adding 58.6 kPa H_2 to 117.9 kPa H_2 shifts the peak by about 20 °C.

Changes in peak shape become significant at the higher deuterium pressures shown in Figure 10. This is related to a blanketing effect resembling that seen with helium. While both hydrogen and deuterium can be absorbed by the palladium, hydrogen is absorbed preferentially. At equilibrium, the molar ratio H:D may be 2 or 3 times higher in the solid than in the gas.[17] The extra hydrogen required by the solid will initially decrease the concentration of hydrogen above the solid, leaving a blanket of deuterium-rich gas, and shifting the local equilibrium. Eventually, more hydrogen gas will be transported into the capsule so that the solid is in equilibrium with the external gas. However, the blanketing effect can still disrupt the heat flow, and produce a distorted peak shape.

Simulations shown in Figure 10 show qualitative agreement with the experiments. The peak positions change only slightly until a concentration of about 10% deuterium in hydrogen, and the peak shape becomes quite distorted as the deuterium partial pressure becomes close to the hydrogen partial pressure. The peak positions for the simulated gas mixtures differ from experimental values by amounts similar to those for pure gases, providing a measure of success for our model of chemical potentials.

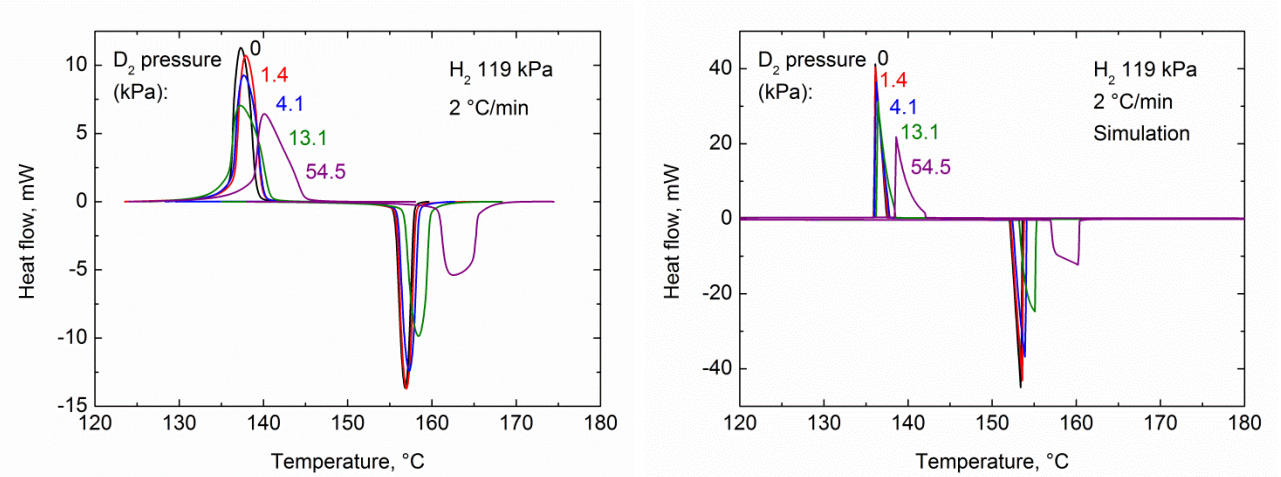

Figure 10. (Left) Calorimetry peaks from titrations of deuterium gas into a fixed partial pressure of hydrogen. (Right) Simulations of the experiments.

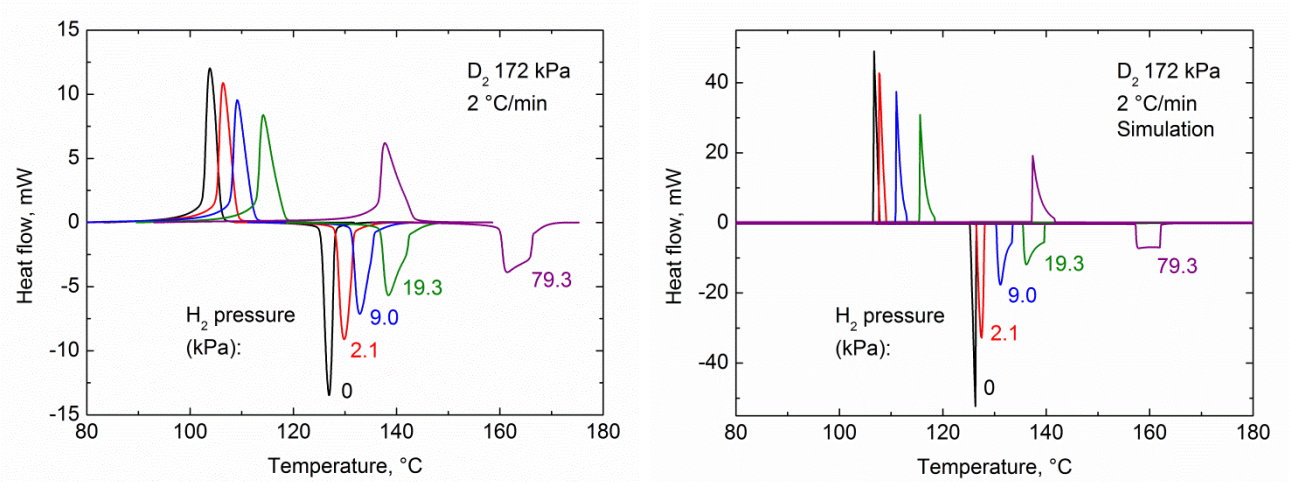

Figure 11. (Left) Calorimetry peaks from titrations of hydrogen gas into a fixed partial pressure of deuterium. (Right) Simulations of the experiments.

For the opposite case, where hydrogen is titrated into a fixed partial pressure of deuterium, the peak shifts are greater than would occur in the case of pure deuterium, and the peak shapes evolve similarly to the previous case, as shown in Figure 11. The simulated peak shapes have sharper corners than the measured peaks, but the overall shapes and widths are similar. The dependence on scan rate of the hydrogen-deuterium mixtures is shown in Figure 12. The shifts in peak position and shape more closely resemble those of the pure gases (Figure 6) than those of mixtures of a pure isotope with helium (Figure 8), suggesting that the blanketing effect is less pronounced in this case.

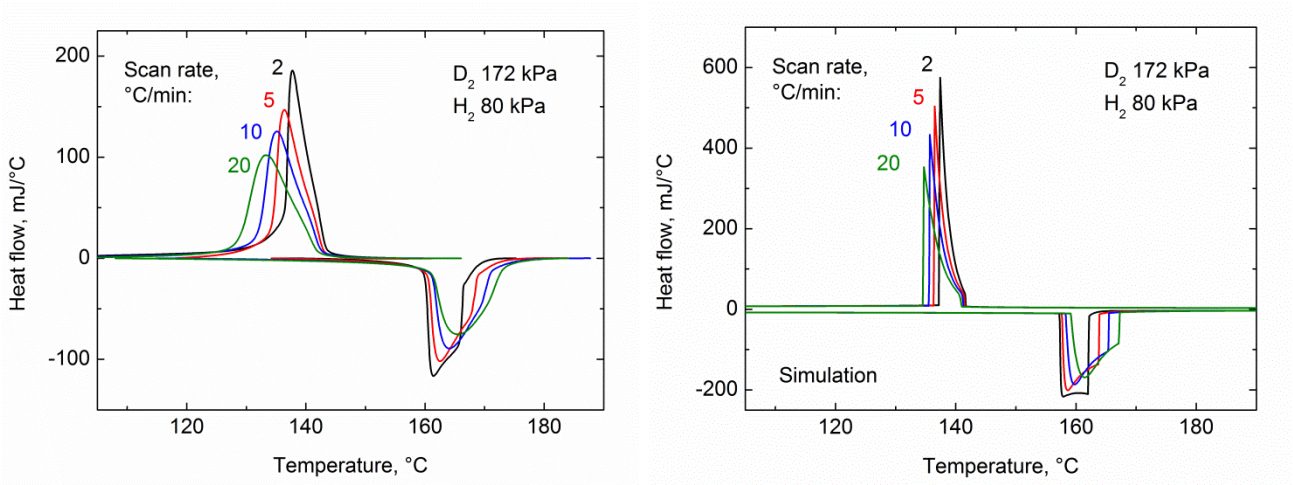

Figure 12. (Left) Dependence of normalized peak shape on scan rate for a hydrogen-deuterium mixture. (Right) Simulations of the experiments.

Clues to the origin of the distorted peak shapes appear in Figure 13, which shows the gas concentrations in the capsule and the hydrogen isotope concentrations in the metal during the course of a simulation. This enables a more detailed understanding than could be obtained from the experimental results alone. There is initially a greater ratio of hydrogen to deuterium in the solid than in the gas phase. During desorption, both species come out of the solid, and the gas-phase ratio approaches the initial solid-phase ratio, which was more hydrogen-rich. When the gas becomes more hydrogen-rich, the desorption temperature moves upward, but not as much as for the case of the hydrogen-helium mixtures. Transport through the hole in the lid limits the accumulation of hydrogen in the capsule. Eventually all of the material in the solid desorbs, but the desorption peak is broadened and distorted. At the onset of the peak, the deuterium comes out of the solid more rapidly than the hydrogen, resulting in peak shapes that increase abruptly, change gradually, and then decrease abruptly, in contrast to the hydrogen-helium desorption peak shapes that increase gradually and then decrease abruptly.

The absorption process is not a trivial reversal of this. The solid absorbs a greater ratio of hydrogen than deuterium as before, causing the gas in the capsule to become deuterium-rich, which further causes the solid to absorb more deuterium than it otherwise would. The heat flow associated with the peak is primarily due to absorption up to its total capacity of hydrogen isotopes. When the palladium first reaches its total capacity of hydrogen isotopes, the heat flow drops sharply. The solid is then at a nonequilibrium composition, because the gas in the capsule is deuterium-rich. However, on a timescale longer than that of the peak, hydrogen diffuses into the capsule and exchanges with the deuterium in the solid, a process that releases an amount of heat near the baseline. This contrasts with the case of the hydrogen-helium mixtures, where the slow diffusion process contributes to a broad peak, especially at high scan rates. As a net effect of the changes in concentration and absorption/desorption pressures, palladium is less isotopically selective when absorbing gas than when desorbing it. This kinetic effect explains the observed difference between the absorption and desorption peak shapes.

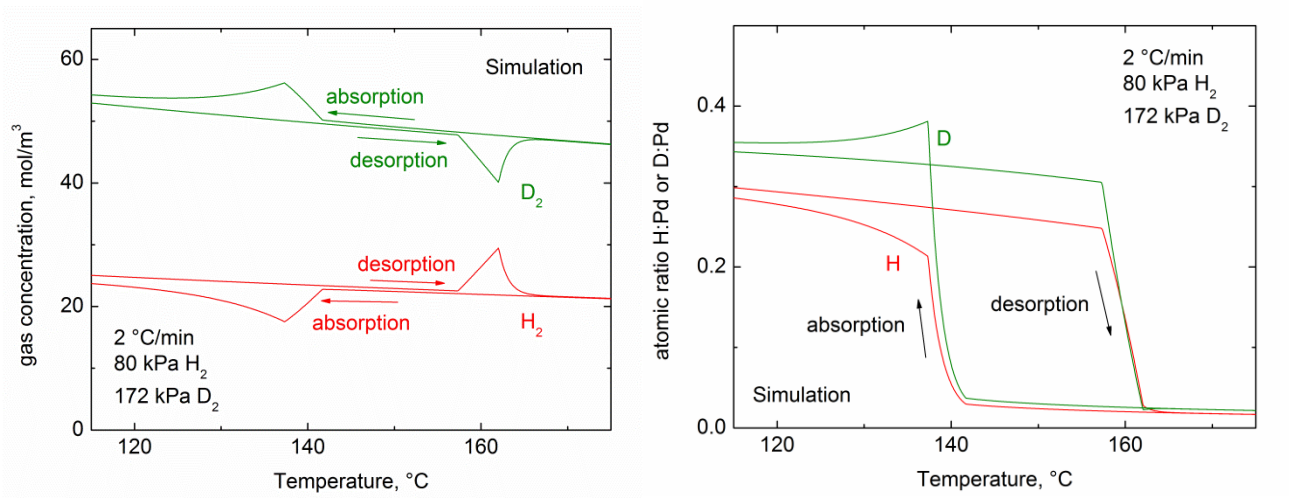

Figure 13. Gas concentrations (left) and hydride concentrations (right) for the 2 °C/min curve in Figure 12. The accounting for gas-phase HD is described in the Modeling Methods section.

The simulations give us confidence that we can understand and confidently predict the results of the calorimetry experiments. They also allow for rapid prediction of results of experiments that are less straightforward to perform than those reported here. Figure S5 in the Supplementary Material shows simulations of calorimetry experiments performed at constant pressure but varying composition. Preparing gas mixtures for such experiments to precise specifications is relatively difficult, but the simulations clearly illustrate the expected sensitivity of the peak positions and shapes to composition, and suggest that changes of isotopic composition by about 1% are distinguishable. Below this level, the model predicts that peak positions differ by a small fraction of the peak widths.

Further analysis of the experimental data can provide approximations of Figure S5 that provide a clearer understanding of the sensitivity of the measurement. Figure S6 replots the experimental data in Figures 10 and 11, normalizing the temperature scales to the peak temperatures for pure hydrogen T_H as predicted by Equation 17. On such a scale, added deuterium shifts peaks to lower T/T_H ratios, and added hydrogen shifts peaks to higher ratios. The peak shifts relative to peak widths are slightly smaller than those in the simulation, but changes of about 1% are distinguishable. While the experiments of Figures 10 and 11 emphasized the ends of the composition range, Figure S6 also shows experimental results for changes in composition of about 1% in the middle of the composition range. These small additions of deuterium shift peaks to lower T/T_H ratios, and small additions of hydrogen cause no distinguishable shift, or small shifts to higher ratios. If we did not know whether this added gas was deuterium or hydrogen, these experimental results would reveal this information. A more detailed effort to optimize the design so that peaks are sharper, such as reducing the heat capacity or improving the thermal conductance of the capsule, could allow for improvements in sensitivity to changes in composition.

Simulations can also conveniently address the case of ternary gas mixtures containing fixed partial pressures of H_2 and D_2, but varying amounts of helium. The simulations shown in Figure S7 predict that sufficient amounts of helium result in peak shapes resembling binary H_2-He mixtures, but peak onsets similar to the helium-free binary H_2-D_2 mixture. This suggests that the peak shape, peak onset, and total pressure can be used to deduce the partial pressures of all three components in a mixture where the mole fractions are otherwise unknown. The simulations presented here each require about two seconds on a desktop computer. The deduction process might require iteration of the simulation to identify a composition that best fits experimental data, which could take substantially longer, but steps could also be taken to optimize the process, such as use of prior data or a coarser model to estimate the solution and avoid simulation of regions away from peaks.

Despite the numerous assumptions, the model predicts the experimental results to a useful degree of accuracy, and allows for a greater understanding of the mechanism of the process by allowing us to estimate the time evolution of gas concentrations, which are not easily measured in the experiments.

4.4 Implications for sensing

The range of partial pressures that could be deduced from calorimetry of a reversible solid hydride depends on the material properties and the available temperature range. At room temperature, based on Equation 16, palladium absorbs hydrogen when its partial pressure is above about 2 kPa, and it absorbs deuterium when its partial pressure is above about 8 kPa. Temperatures near 300 °C are needed to desorb hydrogen or deuterium when their partial pressures are near the critical-point pressures of about 2 or 4 MPa, respectively.[19] Because there is no phase transition above the critical point, we would not expect to observe sharp peaks in calorimetry experiments. These values approximate a valid pressure range for our experimental configuration. For these temperatures, the pressure range can be adjusted by using other sorbent materials such as alloys of palladium with silver or rhodium.[19] An apparatus that can cool to sub-ambient temperatures could be envisioned that would allow study of lower partial pressures. For temperatures and pressures that go significantly beyond those shown in Figure S3, or for different sorbent materials, further experimental validation of the model of the phase diagram of the sorbent material would be necessary.

If the isotopic mixture included tritium, there are several additional considerations. The difference in desorption temperatures for the same pressure of pure tritium and pure hydrogen (or the ratio of pressures at a given temperature) is greater than that between pure deuterium and pure hydrogen,[22] so we could expect improvements in sensitivity for hydrogen-tritium mixtures as compared to the hydrogen-deuterium mixtures studied here. However, the difference between pure tritium and pure deuterium is significantly smaller, so a lower sensitivity could be expected for deuterium-tritium mixtures. A further effect of tritium is its decay heat, although this is quite small, and would be difficult to distinguish from the baseline. The decay heat is about 1 W/mol,[42] and 10 mg Pd can hold about 60 µmol tritium. The resulting 60 µW is about 1% of the typical peak powers measured in this work, and below the baseline values observed in Figures S2 and S4.

For real-time monitoring of composition in an industrial or laboratory process, it is also desirable that we be able to make fast measurements. The experimental desorption and absorption peaks reported above require approximately one minute to collect, and this can be much longer for mixtures that result in broad peaks. If we could scale down the size of the capsule, the measurements could be performed more quickly, because the temperature can be changed more rapidly while maintaining a uniform temperature throughout the capsule. In other words, the thermal conductance generally decreases less rapidly than heat capacity as sample volume decreases. Multiple array elements in a microfabricated device would allow us to perform a parallel search for the desorption temperature, so that at any given time, at least one array element will be absorbing or desorbing the isotope – in effect, replacing time multiplexing with spatial multiplexing.

Scaling down the sample size is a promising approach to improving response time. However, specific parts of the sample may present challenges. The proper scaling of the orifice diameter must be determined; it probably need not decrease in proportion to the sample volume or mass. Our mathematical model is a promising design tool for this. Another consideration is the chemical kinetics of hydrogen uptake and release. If the chemical steps of surface dissociation of diatomic gas molecules or surface-to-bulk absorption are not fast enough, no improvement of response time could be obtained by reducing sample size. Methods to improve reaction kinetics have been described.[43]

5. Conclusions

Differential scanning calorimetry of palladium powder within a flow-restricted capsule is a potentially useful approach to quantifying the atomic composition of binary mixtures of hydrogen, deuterium, and helium. In pure hydrogen or deuterium, calorimetry experiments yield relatively sharp desorption and absorption peaks at temperatures that can be described by a conventional empirical fit. The peak width is influenced by the rate at which gas can flow through the restriction; a pressure buildup shifts the equilibrium desorption temperature in a

manner that opposes further desorption or absorption. The finite rate of chemical reaction kinetics of absorption may also contribute to peak widths at lower temperatures. Helium causes a broadening of hydrogen peaks by shifting the desorption temperature as the gas composition in the capsule temporarily changes during desorption or absorption. This is a mechanism by which the gas-phase mole fraction of helium can be quantified. Hydrogen-deuterium mixtures show shifts of peak positions as compared to the same total pressure of pure hydrogen or deuterium, and a limited amount of peak broadening. The gas that initially absorbs into or desorbs from the palladium differs from the equilibrium composition, resulting in unique peak shapes for each case. If the total pressure is known, it should be possible to deduce the previously unknown atomic composition of a hydrogen-deuterium mixture from calorimetry experiments, within about 1%. Simulations suggest that atomic compositions of ternary hydrogen-deuterium-helium mixtures could be deduced. It may also be possible to use other pairs of hydrogen isotopes that include tritium.

The results for the gas mixtures are reasonably well predicted by a model that accounts for the phase behavior of palladium-deuterium-hydrogen mixtures, and mass transport into the gas and solid phases of the sample capsule. The model is expected to be helpful for the deduction of previously unknown atomic compositions, and for the design of new experimental geometries that may provide improved measurement times or sensitivity. These efforts may ultimately lead to a practical sensor that will allow greater knowledge and control of chemical processes that make use of hydrogen isotopes.

6. Acknowledgements

The authors thank W. G. Wolfer for helpful advice on the use of chemical potentials to derive the pressure-composition isotherms. Sandia National Laboratories is a multi-program laboratory managed and operated by Sandia Corporation, a wholly owned subsidiary of Lockheed Martin Corporation, for the U.S. Department of Energy's National Nuclear Security Administration under contract DE-AC04-94AL85000.

7. References

[1] Malinowski ME, Stewart KD, Verberkmoes AA. FASTGAS: Fast Gas Sampling for Palladium Exchange Tests. Livermore (CA): Sandia National Laboratories; 1991. Report No.: SAND91-8220.
[2] Titov VV. Isotopic quadrupole mass spectrometry of hydrogen and helium, J Radioanal Nucl Chem 1993;174:205-22.
[3] Lee J, Spadaccini CM, Mukerjee EV, King WP. Differential scanning calorimeter based on suspended membrane single crystal silicon microhotplate. J Microelectromech Sys 2008;17:1513-25.
[4] Greve A, Olsen J, Privorotskaya N, Senesac L, Thundat T, King WP, et al. Micro-calorimetric sensor for vapor phase explosive detection with optimized heat profile. Microelectron Eng 2010;87:696-8.
[5] Spadaccini CM, Mukerjee EV, Lee J, King WP. Suspended membrane single crystal silicon micro hotplate for differential scanning calorimetry. In: Proceedings of IEEE 22nd International Conference on Micro Electro Mechanical Systems; 2009 Jan 25-29; Denver, CO; IEEE: 2009. p. 136-9.
[6] Krystian M, Setman D, Mingler B, Krexner G, Zehetbauer MJ. Formation of superabundant vacancies in nano-Pd-H generated by high-pressure torsion. Scr Materiala 2010;62:49-52.
[7] Berlouis LEA, Hall PJ, MacKinnon AJ, Wark AW, Manuelli D, Gervais V, et al. The decomposition of electrochemically loaded palladium hydride: a thermal analysis study. J Alloys Compd 1997;253:207-9.
[8] Kohlmann H. Hydrogenation of palladium rich compounds of aluminium, gallium, and indium. J Sol St Chem 2010;183:367-72.
[9] Artman D, Flanagan TB. Desorption of Hydrogen from Palladium and Palladium-Silver Alloys followed by Differential Scanning Calorimetry. Can J Chem 1972;50:1321-4.
[10] Ponthieu M, Calizzi M, Pasquini L, Fernandez JF, Cuevas F. Synthesis by reactive ball milling and cycling properties of MgH_2-TiH_2 nanocomposites: Kinetics and isotopic effects. Int J Hydrogen Energy 2014;39:9918-23.
[11] Imamura H, Yoshihara K, Yoo M, Kitazawa I, Sakata Y, Ooshima S. Dehydriding of Sn/MgH_2 nanocomposite formed by ball milling of MgH_2 with Sn. Int J Hydrogen Energy 2007;32:4191-4.
[12] Tokoyoda K, Ichikawa T, Miyaoka H, Evaluation of the enthalpy change due to hydrogen desorption for M-N-H (M = Li, Mg, Ca) systems by differential scanning calorimetry. Int J Hydrogen Energy 2015;40:1516-22.

[13] Susic MV, Solonin YM, Kinetic and thermodynamic investigation of hydrogen absorption by ternary $LaNi_4Al$ and $LaNi_4Al$-Pd alloys. Int J Hydrogen Energy 1991;16:271-6.
[14] Leardini F, Fernandez JF, Bodega J, Sanchez C. Isotope effects in the kinetics of simultaneous H and D thermal desorption from Pd. J Phys Chem Solids 2008;69:116-27.
[15] Luo W, Cowgill D, Causey R, Stewart K. Equilibrium isotope effects in the preparation and isothermal decomposition of ternary hydrides $Pd(H_xD_{1-x})_y$ ($0 < x < 1$ and $y > 0.6$). J Phys Chem B 2008;112:8099-105.
[16] Luo W, Cowgill DF, Causey RA. Equilibrium isotope effect for hydrogen absorption in palladium. J Phys Chem C 2009;113:20076-80.
[17] Luo W, Cowgill DF, Flanagan TB. Separation factors for hydrogen isotopes in palladium hydride. J Phys Chem C 2013;117:13861-71.
[18] Fukada S, Minato H, Nishikawa M. Recovery of hydrogen isotopes from inert gas mixtures with a titanium particle bed. Int J Hydrogen Energy 1996;21:741-7.
[19] Flanagan TB, Oates WA. The Palladium-Hydrogen System. Annu Rev Mater Sci 1991;21:269-304.
[20] Fukada S, Samsun-Baharin M, Fujiwara H. Hydrogen absorption-desorption cycle experiment of Pd-Al_2O_3 pellets. Int J Hydrogen Energy 2002;27:177-81.
[21] Knapton AG. Palladium alloys for hydrogen diffusion membranes. Platin Met Rev 1977;21:44-50.
[22] Lässer R. Palladium-tritium system. Phys Rev B 1982;26:3517-9.
[23] Borchardt HJ, Daniels F. The application of differential thermal analysis to the study of reaction kinetics. J Am Chem Soc 1957;79:41-6.
[24] O'Neill MJ. Measurement of exothermic reactions by differential scanning calorimetry. Anal Chem 1975;47:630-7.
[25] van der Plaats G. A theoretical evaluation of a heat-flow differential scanning calorimeter. Thermochim Acta 1984;72:77-82.
[26] Sandu C, Singh RK. Modeling differential scanning calorimetry. Thermochim Acta 1990;159:267-98.
[27] Sandu C, Singh RK. Physical transformations in differential scanning calorimetry. Thermochim Acta 1988;132:89-99.
[28] Wunderlich B. Temperature-modulated calorimetry in the 21st century. Thermochim Acta 2000;355:43-57.
[29] Zielenkiewicz W. How do the mathematical models of calorimeters really work? Thermochim Acta 2004;420:23-7.
[30] Danley RL. Comparison of simulated and actual DSC measurements for first-order transitions. Thermochim Acta 2004;409:111-9.
[31] Dong HB, Hunt JD. A numerical model of a two-pan heat flux DSC. J Therm Anal Calorim 2001;64:167-76.
[32] Eaton JW et al. GNU Octave, http://www.octave.org
[33] Lacher JR. A theoretical formula for the solubility of hydrogen in palladium. Proc R Soc Lond A 1937;151:525-45.
[34] Joubert JM, Thiebaut S. Thermodynamic assessment of the Pd–H–D–T system. J Nucl Mater 2009;395:79-88.
[35] Joubert JM, Thiebaut S. A thermodynamic description of the system Pd–Rh–H–D–T. Acta Mater 2011;59:1680-91.
[36] Oates WA, Lässer R, Kuji T, Flanagan TB. The effect of isotopic substitution on the thermodynamic properties of palladium-hydrogen alloys. J Phys Chem Solids 1986;47:429-34.
[37] Wolfer WG, Meyer BA, Fisher KJ. The vibrational, elastic and electronic contributions to the chemical potentials of hydrogen isotopes in palladium. In: Moody NR, Thompson AW, Ricker RE, Was GS, Jones RH, editors. Hydrogen Effects on Material Behavior and Corrosion Deformation Interactions. International Conference on Hydrogen Effects on Material Behavior and Corrosion Deformation Interactions; 2002 Sep 22-26; Moran, WY. Warrendale, PA: Minerals, Metals and Materials Society; 2003, p. 107-16.
[38] Lässer R, Powell GL. Solubility of H, D, and T in Pd at low concentrations. Phys Rev B 1986;34:578-86.
[39] Flanagan TB, Kuji T, Oates WA. The effect of isotopic substitution on the α-α' phase transition in metal-hydrogen systems. J Phys F 1985;15:2273-81.
[40] Lässer R, Klatt KH. Solubility of hydrogen isotopes in palladium. Phys Rev B 1983;28:748-58.
[41] Flanagan TB, Oates WA. The palladium-hydrogen system. Annu Rev Mater Sci 1991;21:269-304.
[42] Pillinger WL, Hentges JJ, Blair JA. Tritium Decay Energy. Phys Rev 1961;121:232-3.
[43] Cappillino PJ, Sugar JD, Hekmaty MA, Jacobs BW, Stavila V, Kotula PG, et al. Nanoporous Pd alloys with compositionally tunable hydrogen storage properties prepared by nanoparticle consolidation. J Mater Chem 2012;22:14013-22.

Supplementary Material

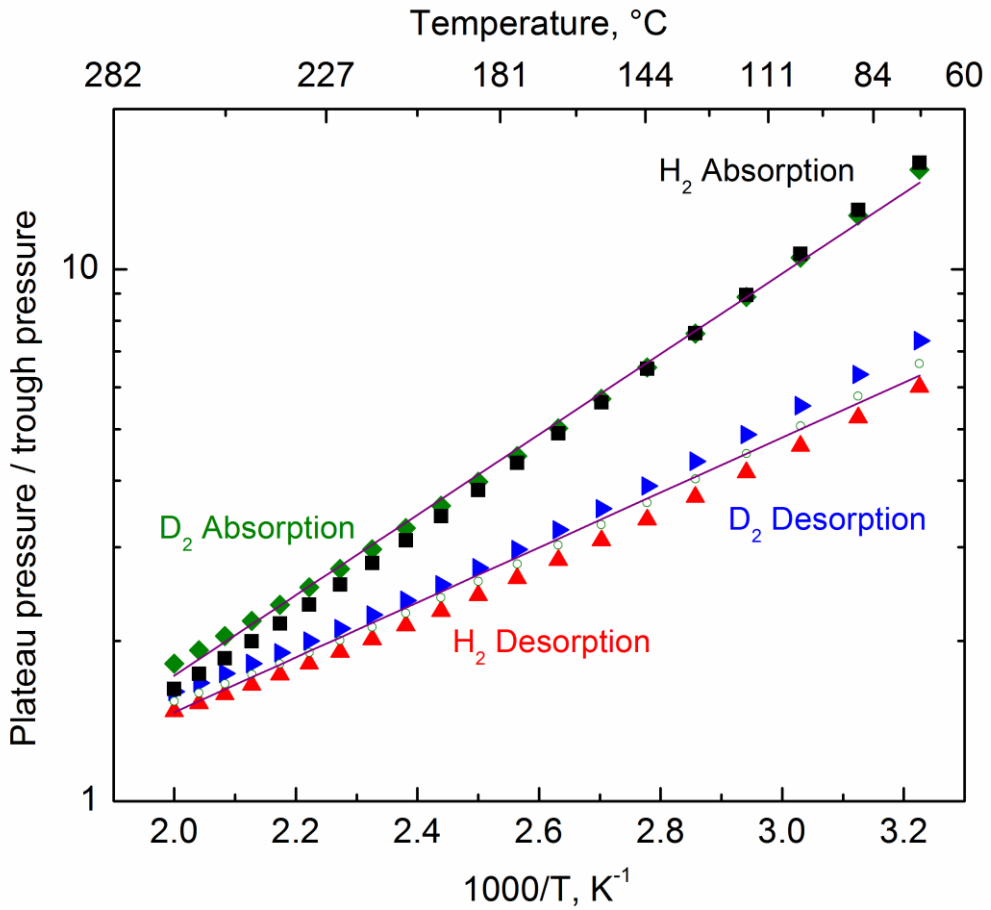

Figure S1. Ratios of pure-gas plateau pressures given by Equation 16 to the trough pressures derived from the chemical potential model (filled symbols); fits to the average of the H_2 and D_2 values for each of absorption and desorption (lines); and the average of the H_2 and D_2 values for desorption (unfilled circles).

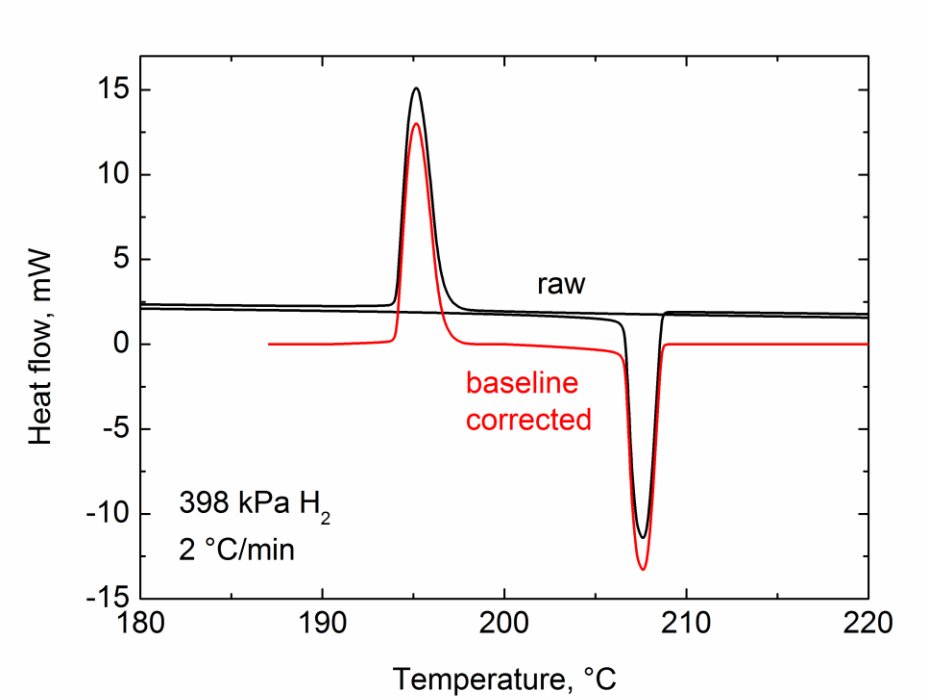

Figure S2. Heat flow versus temperature for a palladium sample in a hydrogen atmosphere, scanned at 2 °C/min, with and without baseline correction.

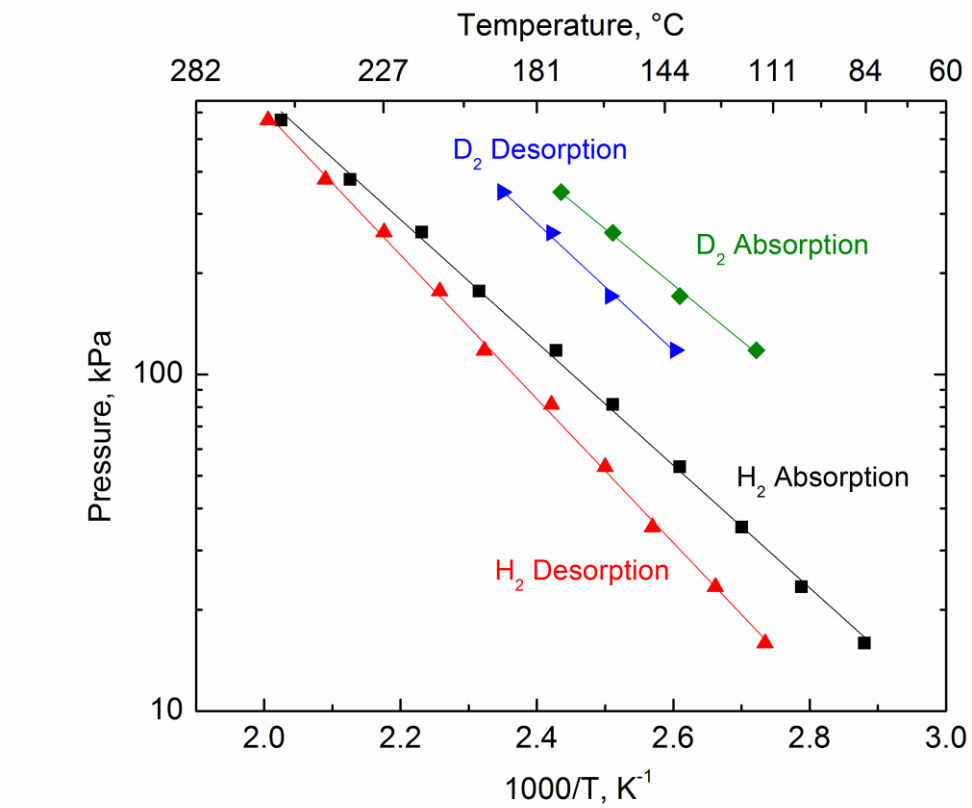

Figure S3. Fits to the peak onsets reported in Figure 5 resulting in the values in Table 1.

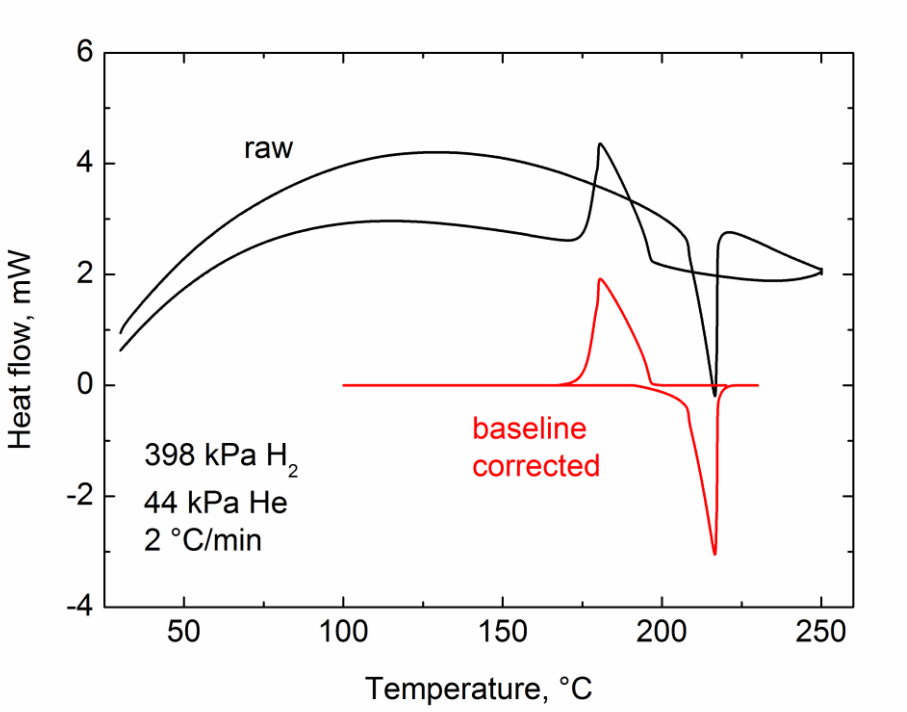

Figure S4. Example of sloped baseline that must be corrected for the case of gas mixtures.

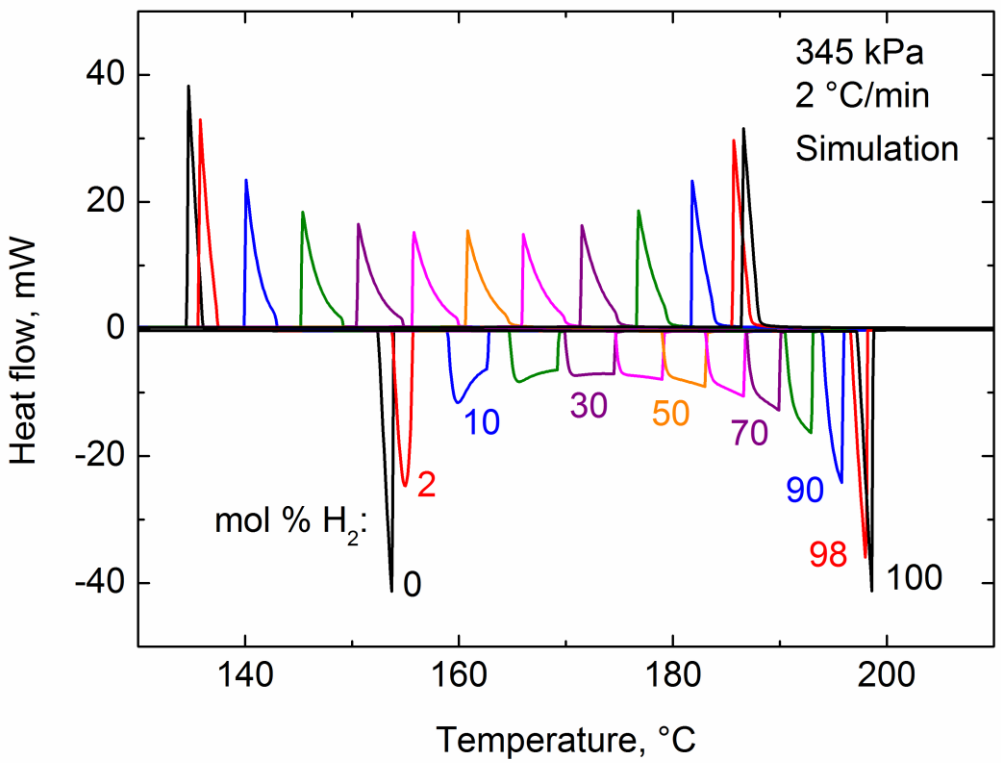

Figure S5. Simulations of calorimetry of hydrogen-deuterium gas mixtures at constant total pressure but varying mole fractions of the gases.

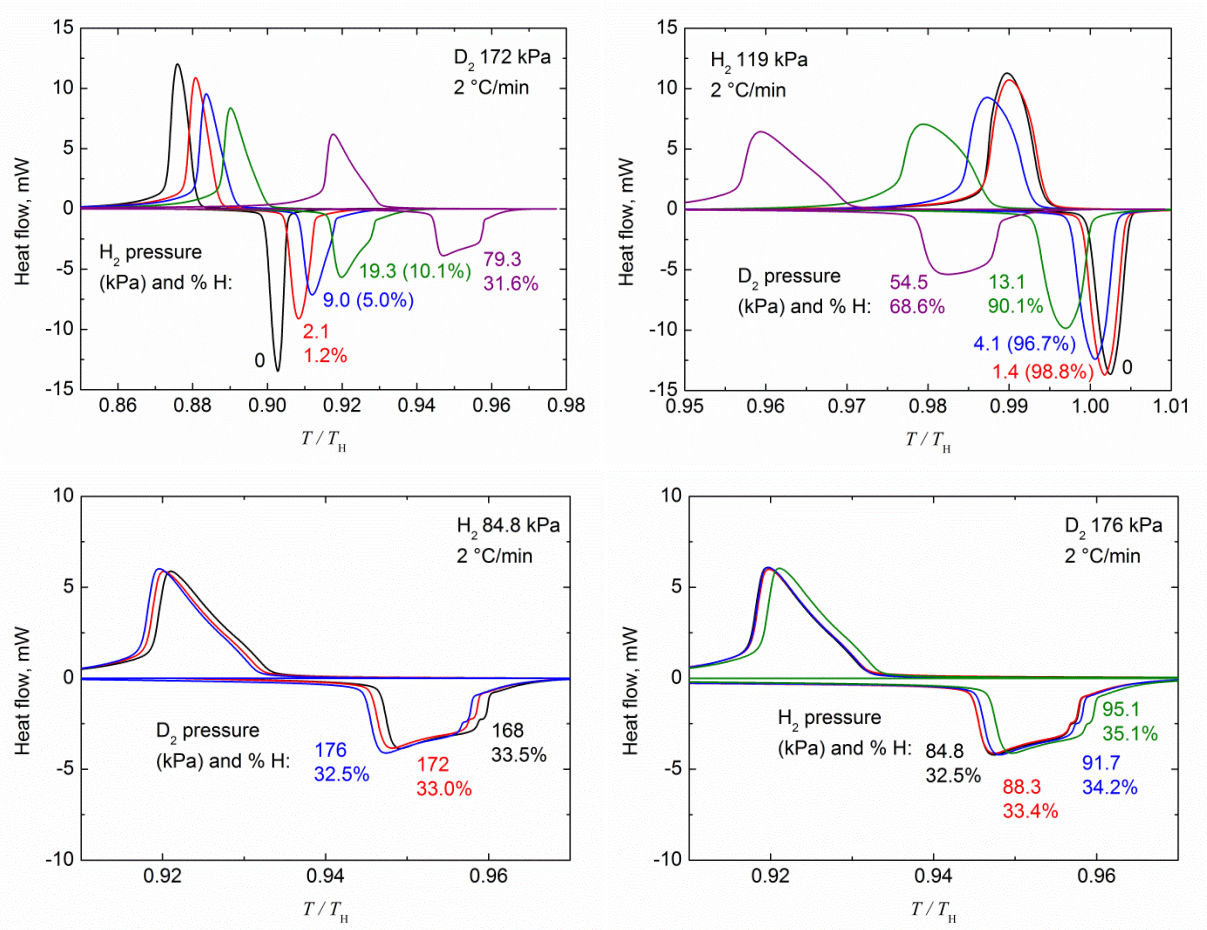

Figure S6. Top: The data in Figures 10(left) and 11(left), plotted versus the ratio of absolute temperature to the pure hydrogen desorption or absorption temperatures, T_H, predicted by Equation 17. The predicted desorption temperatures were used in the ratios for the desorption peaks, and the predicted absorption temperatures were used in the ratios for the absorption peaks. Bottom: similar plots for small additions of (left) deuterium and (right) hydrogen for gas-phase D:H ratios near 2.

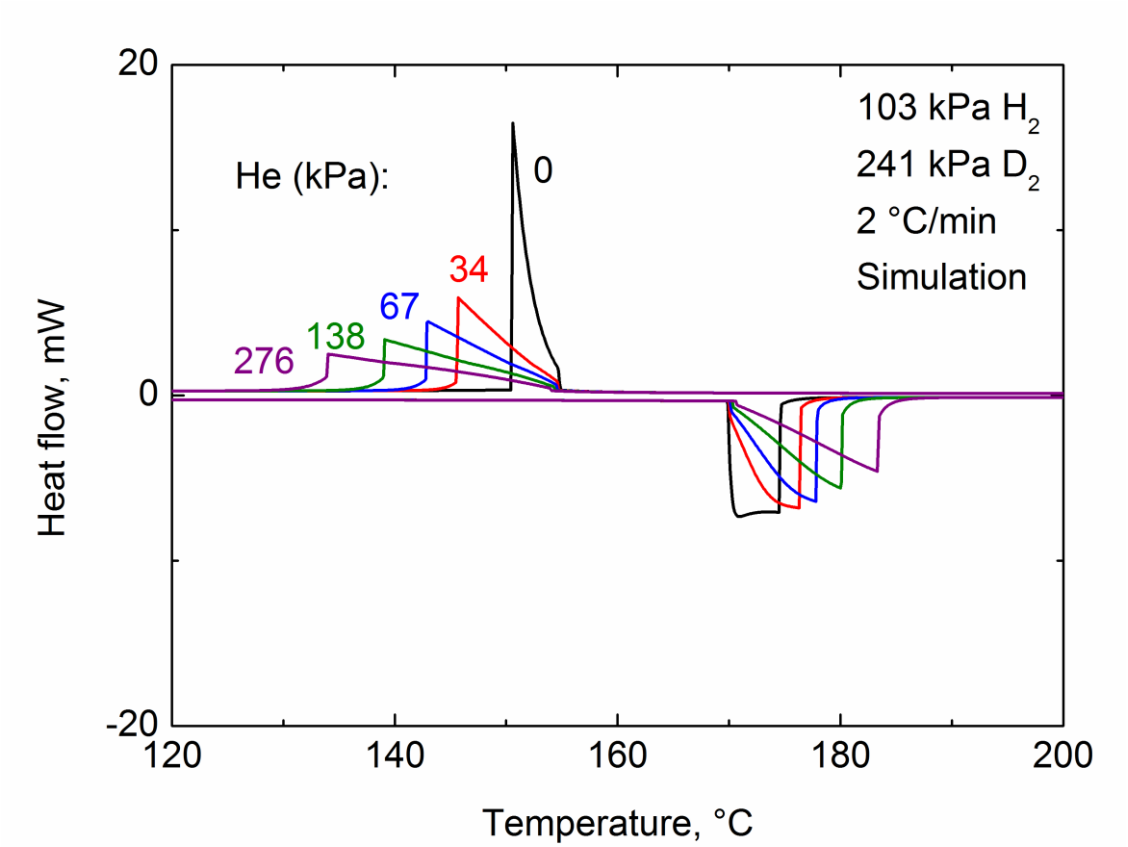

Figure S7. Simulations of calorimetry of a hydrogen-deuterium mixture with varying amounts of added helium.